

Article

Substantiation of Drilling Parameters for Undermined Drainage Boreholes for Increasing Methane Production from Unconventional Coal-Gas Collectors

Boris V. Malozyomov ^{1,*} , Vladimir Ivanovich Golik ², Vladimir Brigida ^{3,4} , Vladislav V. Kukartsev ^{5,6,7}, Yadviga A. Tynchenko ^{8,9}, Andrey A. Boyko ^{7,10,11} and Sergey V. Tynchenko ^{12,13}

- ¹ Department of Electrotechnical Complexes, Novosibirsk State Technical University, 20, Karla Marksa Ave., Novosibirsk 630073, Russia
 - ² Department “Technique and Technology of Mining and Oil and Gas Production”, Moscow Polytechnic University, 38, B. Semenovskaya St., Moscow 107023, Russia; v.i.golik@mail.ru
 - ³ Department of Biomedical, Veterinary and Ecological Directions, RUDN University, 6, Miklukho-Maklaya St., Moscow 117198, Russia; lz011@inbox.ru
 - ⁴ Federal Research Centre the Subtropical Scientific Centre of the Russian Academy of Sciences, Sochi 354002, Russia
 - ⁵ Department of Information Economic Systems, Institute of Engineering and Economics, Reshetnev Siberian State University of Science and Technology, Krasnoyarsk 660037, Russia; vlad_saa_2000@mail.ru
 - ⁶ Department of Informatics, Institute of Space and Information Technologies, Siberian Federal University, Krasnoyarsk 660041, Russia
 - ⁷ Digital Material Science: New Materials and Technologies, Bauman Moscow State Technical University, Moscow 105005, Russia; eboiko@sfu-kras.ru
 - ⁸ Laboratory of Biofuel Compositions, Siberian Federal University, Krasnoyarsk 660041, Russia; t080801@yandex.ru
 - ⁹ Department of Systems Analysis and Operations Research, Reshetnev Siberian State University of Science and Technology, Krasnoyarsk 660037, Russia
 - ¹⁰ Department of Technological Machines and Equipment of Oil and Gas Complex, School of Petroleum and Natural Gas Engineering, Siberian Federal University, Krasnoyarsk 660041, Russia
 - ¹¹ Department of Management, Reshetnev Siberian State University of Science and Technology, Krasnoyarsk 660037, Russia
 - ¹² Department of Digital Control Technologies, Institute of Business Process Management, Siberian Federal University, Krasnoyarsk 660041, Russia; stynchenko@sfu-kras.ru
 - ¹³ Department of Computer Science and Computer Engineering, Institute of Computer Science and Telecommunications, Reshetnev Siberian State University of Science and Technology, Krasnoyarsk 660037, Russia
- * Correspondence: borisnovel@mail.ru



Citation: Malozyomov, B.V.; Golik, V.I.; Brigida, V.; Kukartsev, V.V.; Tynchenko, Y.A.; Boyko, A.A.; Tynchenko, S.V. Substantiation of Drilling Parameters for Undermined Drainage Boreholes for Increasing Methane Production from Unconventional Coal-Gas Collectors. *Energies* **2023**, *16*, 4276. <https://doi.org/10.3390/en16114276>

Academic Editor: Shu Tao

Received: 27 April 2023

Revised: 20 May 2023

Accepted: 21 May 2023

Published: 23 May 2023



Copyright: © 2023 by the authors. Licensee MDPI, Basel, Switzerland. This article is an open access article distributed under the terms and conditions of the Creative Commons Attribution (CC BY) license (<https://creativecommons.org/licenses/by/4.0/>).

Abstract: Decarbonization of the mining industry on the basis of closing the energy generation, on the basis of cogeneration of coal mine methane, and on the internal consumption of the mine is a promising direction in ensuring sustainable development. Known problems of deep underground mining do not allow for realizing the potential of man-made gas reservoirs due to the deterioration of the conditions of development of reserves of georesources. The aim of the work was to improve recommendations for the substantiation of drilling parameters for undermined drainage boreholes for increasing methane production from unconventional coal-gas collectors. The authors’ approach innovation lies in the possibility of using the established patterns of better natural stability of undermined boreholes to optimize them as spatial orientation parameters in an existing drilling passport for the improvement of methane extraction productivity. For this purpose, smoothing (LOESS) of the experimental data of two similar types of wells was used; then deterministic interpolation methods in combination with a three-dimensional representation of the response function in “gnuplot” were used. As a result, it was found that the increase in the inclination angle from 40° to 60° leads to a significant transformation of the model of the studied process, accompanied by a decline in the dynamics of methane emission and a decrease in the distance of the productive work zone of this type of well from 13 to 5 m before the roof landing, which then is replaced by a sharp increase in the productive work zone up to 35 m ahead of the longwall face. This allows under specific conditions for recommending increasing the productivity of methane capex from technogenic disturbed coal-gas

reservoir replacement of wells with a smaller angle of rise to the transition to a more frequent grid of clusters from wells #4.

Keywords: coalbed methane; longwall; gas flow modeling; mining industry decarbonization

1. Introduction

Decarbonization of the extractive industry, as the basis for transforming the energy sector within the circular economy (CE), is one of the promising ways to achieve sustainable development [1,2]. In turn, this circumstance necessitates the improvement of state regulation [3], in the field of both monitoring the distribution of mine methane flows [4] and aerological risk assessment [5], as well as in the humanization of higher education for future mining engineers [6].

Changing the general approach to mine methane as an alternative and more environmentally neutral energy carrier (than coal) implies that gassy coal deposits should be perceived as sources of unconventional coal-gas collectors (due to the presence of technogenically disturbed rock massif). The use of electricity and heat obtained from the cogeneration (trigeneration) of the extracted gas for the internal consumption of the mine allows for obtaining a synergistic effect of reducing the cost of coal mining and the sale of futures to reduce CO₂ emission units and increase the safety of mining. At the same time, in practice, the realization of the given concept is connected with the necessity of the decision on known problems of deep underground mining [7,8]. This is associated not only with geomechanical issues [9–11], but also with the inconsistency of the coming system components, which in turn does not allow for reducing the carbon footprint of the mined georesources [12]. The reduction of emissions of climate-active gases in the process of mining is possible only with the reliable operation of a network of surface cogeneration units [13,14] and the formation of smart “coal–energy–information” systems [15].

The peculiarity of technogenic gas reservoirs is the complication of geomechanical conditions caused by the dynamic component of the support pressure when implemented in the transition from the vault theory (“O” circle theory) [16–18] to more advanced theories, taking into account the phenomenon of Oparin’s “zonal disintegration” of rocks, a discrete and fractal array in the area of lead fracturing [19–22] (probably with the account of the mathematical apparatus of nonlinear dynamics—solitons, attractors). One of the most debatable areas is the prediction of zones with different parameters of the filtration channels “methane drainage zone” [23–25], which provide a decaying metastable solid gas-coal solution and the boundaries (angles of complete displacement) [26–29] for real conditions of reserve development. For this purpose, a commercial software, which implements numerical simulation methods, such as the finite element method (FEM) in COSFLOW [30,31], CFD gas flow in ANSYS [32,33], CMG-GEM [34], PFC2D [35], finite differential method (FDM) in FLAC3D [36], discrete models [37] (such as UDEC [38,39]), and physical simulation with equivalent materials [40], is widely used. At the same time, valid estimation methodologies are still lacking to fully understand the processes under study. The main patterns of rock pressure manifestations, in our opinion, can be identified and analyzed based on the characteristics of methane concentration dynamics in underground degassing wells drilled on the overlying massif, which can also help explain the mechanism for the development of deformation processes in it.

Approaches to estimating the distribution of gas flows in the mined-out space and the overlying massif are investigated quite comprehensively in works [41–43], while the lack in the theoretical basis of sorption is extended by empirical research methods [44,45]. In addition, one of the promising directions of physical modeling [46–49], when physical gas flows are passed through the equivalent materials subjected to three-axis loading, should be noted. In this case, it is possible to overcome the limitations of empirical–analytical models (for example, based on Allan variation) [50] or three-dimensional regression [51].

At the same time, in the practice of mining, the existing recommendations do not always contribute to ensuring the normative coefficients of degassing efficiency at the mine site. In this connection, the questions of optimization of the parameters of degassing wells at the surface mining of gas-coal formations remain not completely studied. The purpose of this study is to improve recommendations for the substantiation of drilling parameters for undermined drainage boreholes for increasing methane production from unconventional coal-gas collectors.

2. Materials and Methods

The object of the study is the 18th eastern face (length of 305 m, depth of 1300 m) of formation m^3 (thickness of 1.55 m, dip angle of 6° , methane content to $23 \text{ m}^3/\text{t}$ dry ashless mass) of JSC “mine named after AF Zasyadko”. The ventilation drift of the 18th eastern face was undercut to the conveyor drift above the worked-out 17th eastern face, leaving a 2 m interstrip pillar along the whole length of the ventilation drift behind the face, supported by the drift pads, installed along the drift axis, and a 2.0 m wide cast strip, along the worked-out space. To prevent oxidation of the coal pillar, left along the ventilation drift, the coal is constantly treated with a film-forming flame retardant. The system of development includes long columns along the strike, with a panel method of preparation of reserves. The work is carried out according to the one-sided scheme in the direction of the fresh air jet with oblique runs in the lower part of the face. The maximum permissible daily load on the longwall face is 2970 t/day at the air supply to the area— $1548 \text{ m}^3/\text{min}$.

The degassing system of the mine consists of an underground degassing network (a set of various types of underground wells drilled on the panels being mined, interconnected by a 630 mm pipeline; local pipelines are interconnected in the main drift and then go to the surface), a vacuum pumping station (at surfaces for supplying vacuum pressure to the wellhead of each borehole through a pipeline; VVN-150 pumps are used), surface wells drilled into the goaf of the panels being worked out (connected to each other and the vacuum pumping station by pipelines of smaller diameter), a cleaning system and preparation of methane–air mixture and an engine room (surface rooms with 12 JMS 620 gas piston units of the Austrian company Jenbacher), and a surface vacuum pumping station (located at the industrial site of VPS N° 2).

They are switched in the operation in parallel, 2 units for each pipeline (530 and 630 mm in diameter). The degassing network consists of surface and underground wells connected by pipelines, which in turn are connected to the main pipelines coming to the surface. Wells at the considered mine site were combined into alternating “clusters” of two types—two or more degassing wells drilled into the carbonaceous massif near the corresponding picket (S, distance from the object to the beginning of the panel). Type (1) included well type N° 1, 3, and 4, and type (2) included N° 2, 3, and 4. Drilling was carried out with GBH-1/89/12 machines (Germany) ahead of the face at a distance of $L > 60 \text{ m}$. When drilling to the depth of the fractured zone, conductors of $\varnothing = 152 \text{ mm}$ were installed. The methane concentration was measured during the repair shift in a standard way at the wellhead (beginning of the hole) using the catalytic sensor CatEx 125 PR Mining of the Dräger X-AM 2500 gas analyzer.

To assess the influence of the topology of the network of wells on the productivity of degassing of the undermined rock mass, wells were selected—type N° 3 and N° 4 (Table 1). The choice was because their basic parameters were the same except for the angles $\beta = 60^\circ$ and 40° and $\varphi = 60^\circ$ and 35° for wells N° 3 and N° 4, respectively. In the mined-out space, as a protective structure for the drift and degassing wells, a 2 m wide bi-fastener was built (Figure 1). In addition, along the axis of the excavation were wooden bonfires made of stakes 1.5 m long, and the distance between the bonfires 6 m.

Table 1. Borehole parameters.

	Borehole Length (m)	Inclination Angle β ($^{\circ}$)	Hole Azimuth φ ($^{\circ}$)	Hole Diameter (mm)	Casing Diameter (mm)	Casing Length (m)	Drillhole Spacing (m)
N $^{\circ}$ 3	120	40	35	132	120	15	20–25
N $^{\circ}$ 4	120	60	60	132	120	15	20–25

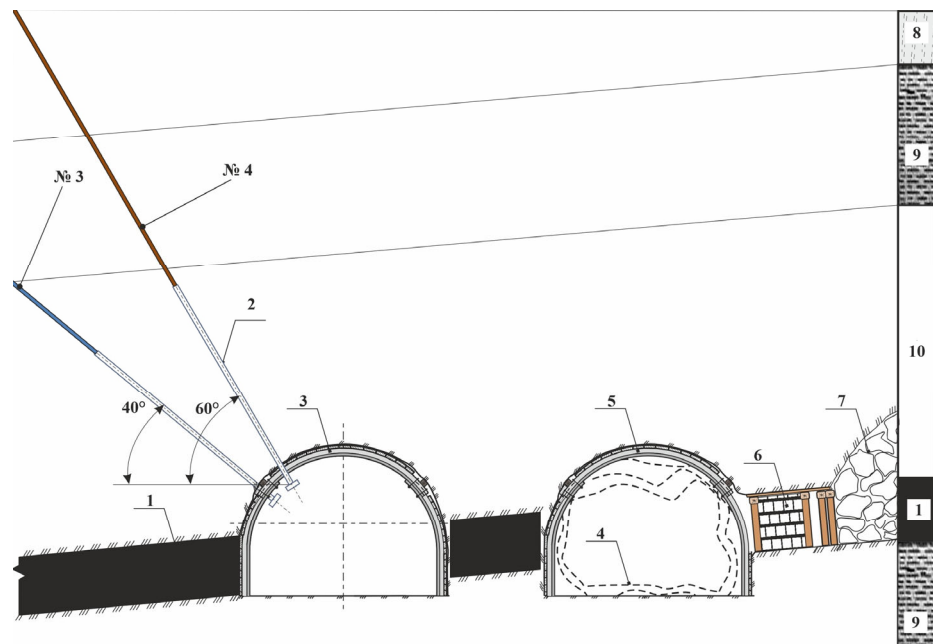


Figure 1. Location of wells N $^{\circ}$ 3 and N $^{\circ}$ 4 in the mine site: 1—coal seam; 2—well casing; 3—air roadway 18th eastern longwall; 4—roadway deformations; 5—haul roadway 17th eastern longwall; 6—lining; 7—goaf; 8—sandstone; 9—aleurolite; 10—claystone.

Spatial analysis of heterogeneous data remains one of the most difficult tasks of predicting the distribution of the response function over the factor space [52], solved using different approaches: fuzzy logic in MATLAB fuzzy logic [53]; stochastic modeling [54–56]; wavelet analysis with the Morlet algorithm (CWT) [57,58]; analytical methods based on using trigonometric relationships for quadratic surfaces [59]; nearest neighbor method [60]; inverse weighted distance (IDW) method [61]; multivariate nonlinear regression in SPSS software, www.ibm.com/spss [62]; and machine learning [63], fuzzy cognitive map (FCM) [64], or artificial neural networks (ANN) [65], using GIS technologies—crunching methods [66–68]. At the same time, deterministic methods of three-dimensional data interpolation have not lost their relevance [69].

Proceeding from the experience of practical working in mine conditions allows for concluding that the quality of the normative forecast turned out to remain low. In most scientific works, two-dimensional curves or their aggregates in the form of projections on a two-dimensional plane are mainly considered [70–73]. For example, a two-dimensional curve characterized by the relationship between the methane concentration and distance S at different times, as well as the methane concentration change over time at different positions, is insufficiently representative (see Figure 2 in [26]) owing to the deformation of a three-dimensional surface when it is projected onto a two-dimensional plane. This conceptual imperfection in the methodological approach does not allow for adequately interpreting the obtained results, not to mention the formation of universal conclusions and generalized regularities. The general formulation of the problem even in the presence of the initial spatial limitation on the number of dimensions (first instead of third) is reflected

insignificantly. Along with the previous studies, CH_4 (the methane concentration in the mouth of underground wells under constant vacuum pressure) as a function of the response from S (distance from the wellhead to the beginning of the panel during its development by reverse stroke—the “space” factor limited by the first dimension) is considered. There is also t (the time of making the measurement), S_L (the position of the face relative to the panel beginning), and S_t (the time at which the face occupies a certain position relative to the panel beginning). The above-mentioned show that this is a five-dimensional task, which, at best, is more correctly displayed by a set of four-dimensional ones. The previous studies made it possible to find approaches to how to lower the dimension during the transition from S_L – S_t to L [74]. This substantially facilitated approaches to identifying the interrelation of the effect of the remoteness from lava on gas flows. In this paper, an attempt was made to establish the inverse problem, which is the impossibility of considering gas flows without the “lava component”, which gradually transforms their dynamics (if we consider the dynamics separately from lava)—“lava influence profile”. In this regard, for the first time, when a four-dimensional space–time problem was considered limitedly (that is, without L in the CH_4 – t plane), according to the planned approach, the parameter S was introduced. This made it possible to consider the process under study as a function (given in the implicit form) of CH_4 of S (the space axes—distance from the beginning of the site “by analogy with the distance from the beginning of the site to the position of the lava in other moments of time”), t (measurement time).

The next important aspect is obtaining a theoretical model [75–77] (process formulas, or a regression having a preset level of “goodness-of-fit”), which is still an open fundamental scientific task for three-dimensional models (see, for example, [78–80]). At this stage, the author’s approach provides for the construction of a model of the response surface most qualitatively (based on the Q – Q curve) reflecting the general regularities of in situ data.

As can be seen from [81], the algorithm for working with data was an alternation of the following sequence of actions: in *Vi Improved*, a Python script was written to filter the primary experimental data using the Savitzky–Golay method (https://docs.scipy.org/doc/scipy-0.16.1/reference/generated/scipy.signal.savgol_filter.html, accessed on 26 April 2023) [82]. At the next stage, one of the standard methods (finite elements) of 3D interpolation of scattered data was considered by Prof. R.J. Renka [74]. Next, in *gnuplot*, a response surface was built for the process under study. At the last stage of the study, Q – Q graphs were built in MS Excel to assess the quality correspondence of the model to experimental data.

Several operators implement a standard b-spline interpolation procedure in the “*gnuplot*” program. To select a color, we used the “set palette gray” operator. The first is «set hidden3d» (The “set hidden3d” is a command that enables a hidden line removal for surface plotting (see *splot*). Some optional features of the underlying algorithm can also be controlled using this command). The second is «set pm3d at bs» (*pm3d* is a *splot* style for drawing palette-mapped 3d and 4d data as color/gray maps and surfaces. It allows for plotting gridded or nongridded data without preprocessing. The *pm3d* style options also influence solid-fill polygons used to construct other 3D plot elements). The third is «set dgrid3d . . . » (the *dgrid3d* command enables and can set parameters for nongrid to grid data mapping). The fourth is the set view options and *xrange*, *yrange*, and *zrange*. The fifth is «*splot* “./2022_Golik_k.txt”». We have not included a detailed description of the algorithm and its implementation script in the application only because of the patent insecurity of the author’s approach (the work is underway).

The field data sets had 175 rows for well #3 and 213 rows for well #4. Examples of data sets for the studied parameters of measurement time (t), distance from the wellhead to the beginning of the picket panel (S), and methane concentration in the discharged gas-air mixture (CH_4) displayed in Table 2.

Table 2. Data on methane concentrations in underground wells.

N	Borehole #4			Borehole #3		
	t, day	S, m	CH ₄ , %	t, day	S, m	CH ₄ , %
1	81	1330	2	81	1330	7
2	81	1310	0	81	1310	15
3	81	1280	0	81	1280	0
4	81	1260	3	81	1260	1
5	83	1330	11	83	1330	14
6	83	1310	1.5	83	1310	14
7	83	1280	0	83	1280	0.5
8	83	1260	1	83	1260	3.5
9	88	1280	3	88	1280	0

3. Results

The response functions of the spatial distribution of gas flows plotted for the raw primary data sets are shown in Figure 2.

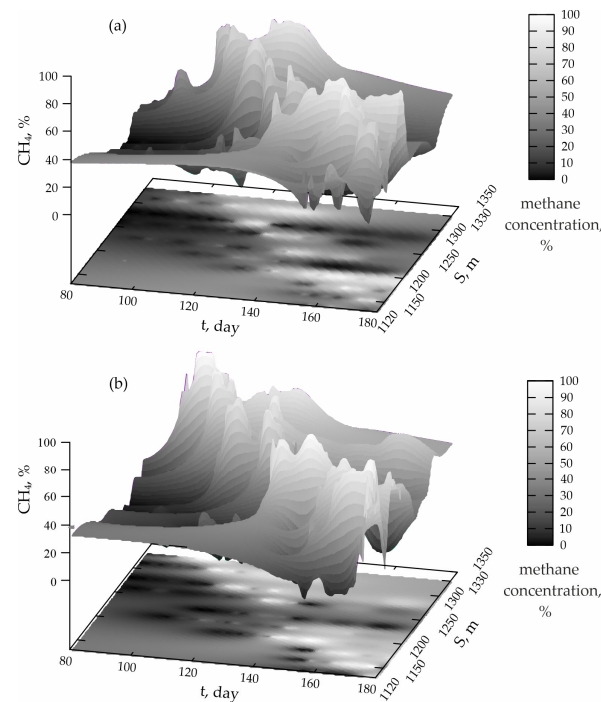


Figure 2. Dynamics of methane emission in “space-time” coordinates based on primary information: (a) and (b)—wells N° 3 and N° 4, respectively.

From the analysis of Figure 2, it follows that the alternation of local maxima and minima occurs along the line of the curve, oriented at a certain angle to the t-S axes. In this case, although not so clearly, this is a reflection of the impact of the stope on the activation of roof shear and the formation of aerological connections between pressure relief zones and goaf. The projections of the zones of maximum gas release in the form of white spots are localized along the conditional line of movement of the face, which began its movement from the upper-left corner (rectangular projection of the response surface) $t = 80$ days, $S = 1330$ m. The entire left part of the projection (from the lower-left corner $t = 80$ days, $S = 1120$ m), painted in gray with dark zones of “low methane runoff” before the start of white spots, represents the zone of operation of the network of wells ahead of the bottom line. Starting from the conditional curve, white spots and to the right of it characterize the features of well operation when their mouths and wellbore protrusions are in the goaf (in that part of the hanging rock consoles where part of their working section remains). As can

be seen from Figure 2, the general picture for both types is characterized by discontinuous contours, which, in our opinion, may indicate the possible discontinuity of the deformation processes that occur in the undermined massif, which are described in detail in [83]. The brighter peaks and their larger size for well No. 4 may indicate a greater efficiency of methane degassing from the degassed massif. At the same time, the sharp features of common surfaces do not allow one to single out the main regularities of the process under study in space–time.

The overall picture of the response surfaces (Figure 2a,b) in the above two cases, from this angle, convincingly proves the fallacy of constructing three-dimensional regression models for raw data (that is, without smoothing and three-dimensional interpolation: filling gaps in the grid data). These facts confirm the correctness of the general methodological approach of the data at this stage for the subsequent comparison of the projections of the response function of models when determining the function type (Fourier, P.L. Chebyshev polynomials, or others). In case of rejecting this approach, the work results would be a qualitative representation of the surface of the “data noise”. In the future, to develop fitting data algorithms, it is necessary to identify “typical lava influence profiles” to understand to what the regression surface should really approach (using the least squares method).

The processing of the initial data according to the above method in combination with the imposition of spline isogases made it possible to concretize Figure 3. Isogases are given with a step of 10% as curves of different colors on the projections of the smoothed and padded data of the studied response surface. Gaps in color on t-S projections characterize the zone with “conditionally zero” concentration of gas in the mixture, if they are located in the “black area”, and the zone of maximum methane output, if they are located in the “white area” (limited by the green curve). From the analysis of Figure 3a, it can be seen that well No. 3 is characterized by a clear alignment of local methane production maxima along the conditional line of bottomhole movement (the direction of which is clearly visible from the surface). Ahead of the bottomhole, one can see the absence of prospects for early gas production by underground wells at a considerable distance from it. The contours of the response surface after a long, stable low section gradually increase as you approach the lava by 20–30 m. After that, the methane emission increases sharply to its maximum, followed by (in most cases) maintaining high values and beyond.

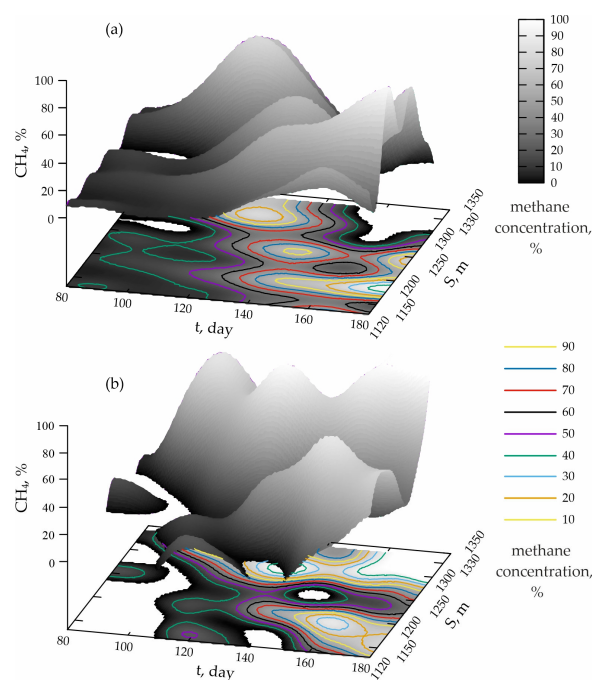


Figure 3. Models of methane emission dynamics for (a) well #3 and (b) well #4.

Behind the lava (to the right of the curve, which can be drawn along the contours of the yellow curves at about 60%), a nonlinear alternation of local maxima and minima can be traced. This can be associated with a number of hard predictable factors for the development of reserves: the slope of the roof, the loss of the stability of wellbores, the discontinuity of the movements of the roof rocks, the uneven mining and geological conditions, etc. It should be noted that at this time, most of the total gas production rate is extracted within the well cycle and most of the negative manifestations and threats to its stable operation.

From the analysis of Figure 3b, it can be seen that well No. 4 is characterized by less predictable behavior with a pronounced staging. The conditional bottomhole approach line is not so pronounced due to the presence of a dark open boundary at 1240–1220 m from the beginning of the panel. It should be noted that this indicates either the collapse of the well (or the inclusion of a well with a blocked wellbore) in the pad or its complete collapse due to the slope of the main roof. The first option is unlikely (from the experience and specifics of the mine); at the same time, a serious break in the productivity of the entire drainage network should be noted due to unfavorable situational and geological conditions for the development of reserves. The subsequent zone of increase in the productivity of the network of wells No. 4 indicates the “interception” of part of the gas flows from more remote wells of this type. Due to the constant supply of vacuum pressure to each wellhead, it was not possible to increase the “vacuum” for more remote wells, which did not allow for improving the safety of work on these days.

The distribution of methane flows is shown in Figure 4. From the analysis of Figure 4, it follows that wells No. 4 are more preferable for advanced degassing purposes. This is due to the fact that their zone of productive work (see yellow curves) begins at the beginning of the development of reserves (left side of the figure) approximately 5–13 m ahead of the face; after the landing ledge, the roof remains solid, reaching 20–35 m. For wells No. 3, discontinuous zones of local maxima are visible both in front of and behind the longwall, and the yellow curve (at the beginning of mining) is below the longwall movement line no more than 5 m. In addition, after, the roof exits sharply and, in some places, increases up to 40 m. Based on this, it can be argued that this type is more sensitive to changes in the stress–strain state of the coal massif and, as a result, is less reliable in the operation.

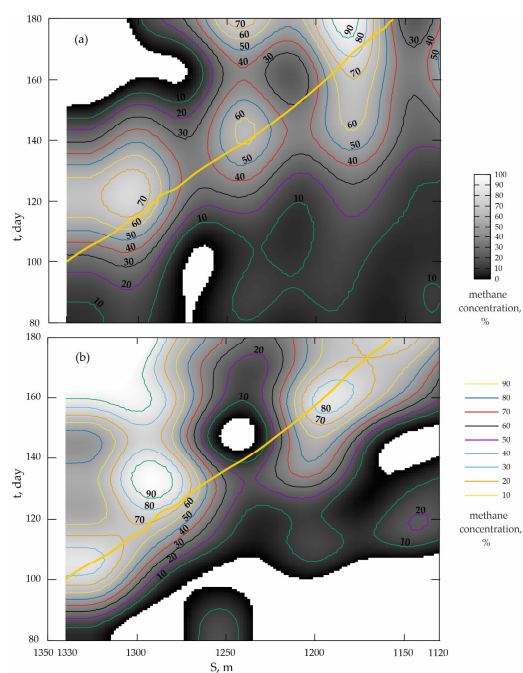


Figure 4. Evolution of methane concentration during degassing of the undermined rock mass: (a) is well #3 and (b) is #4 (the thickened curve is the line of face movement).

If in the area of operation, immediately before sowing the roof in well No. 3, the maximum concentration of methane was about 70% and began in the area with a stope, then for well No. 4 under the same conditions, the maximum already reached 90% and was starting from 10 to 15 m in the worked-out space. The lower natural stability in well No. 3, however, allowed the drainage network to work more stably (presumably due to better interception of gas flows from the fractured zone by remote wells during roof seeding). Due to the sharper elevation angle (40°), most of the massif can be “intercepted” in the event of failure of any of the wells. The results of the Q–Q plots are shown in Figure 5.

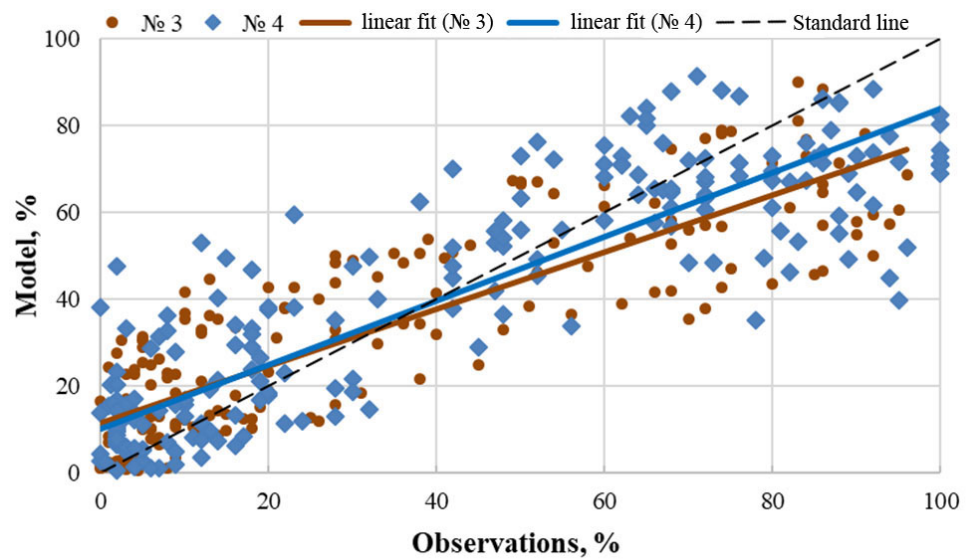


Figure 5. Quality of gas flow modeling based on residual analysis.

The analysis of Figure 5 shows that the linear trend for the model data for well #3 is slightly more deviated from the black line, to the quality of which it is necessary to strive. The linear trend equation has the following form ($R^2 = 0.71$):

$$M = 0.659O + 11.36 \quad (1)$$

In addition, from Figure 5, it is obvious that the model data for well #4 have minimal deviations from the black line, and the angle of slope of the blue line is slightly less than for well #3 (which can be explained by the difference in sample volumes for the studied datasets). The linear trend equation has the following form ($R^2 = 0.76$):

$$M = 0.738O + 10.02 \quad (2)$$

From the analysis of the slope angles of the linear trends and the parameters of the obtained equations, we should say that the quality of the obtained models is satisfactory.

4. Discussion

The average flow rates of the two considered wells were close in absolute values and strongly depended on the position of the longwall face. Like the concentration of methane, the net gas flow rate before the longwall was 0.8 to 1.3 m/min (on average 0.6 m/min); after the passage of the longwall, the wellhead point varied from 2.5 to 2.9 m/min (in some cases reaching 4–5 m/min). The most important factor for maintaining productive work and the safety of the wellbore was the manifestation of rock pressure. From the analysis of Figure 4, it follows that wells No. 4 (see the response surface projection in Figure 4b) are more productive. This is manifested in the fact that, compared with type No. 3, wells of this type have a uniform and sufficiently large distance from the crest of the local maximum (50–60% curves) to the face (below the thick yellow line is the position of the face at each

point in time). This is a consequence of the fact that the wells generally work better with the development of situational geomechanical conditions in the extraction area compared with the more “nervous” behavior of less stable wells No. 3. Zones of maximum methane release in type No. 3 are more localized and unevenly distributed along the length of the yellow line. At the same time, during the primary roof breaks, they do not completely fail.

From the analysis of the obtained models, it follows that after the borehole collapse zone, the angle of methane release in front of the face increases, which indirectly may confirm the formation of a new hanging console of rocks due to established roof breaks [84]. The temperature profile of the production string is important for ensuring wellbore sustainability, which, with a lack of control, can lead to packer sealing failure [85]. Besides, we should admit the growth of the stability problem (borehole collapse and shrinkage) [86–88] for wells N° 3 and N° 4 by the mechanism described in [89,90]. Some cases of productivity loss in the operation of the degassing network at a mine site are caused by imperfect drilling techniques [91,92] or the limitation of downhole methods of resource extraction by surface boreholes [93–95]. In this case, it is rather worth recognizing the insufficient rigidity of the security structures erected in the goaf [96]. In some cases, the theory and mechanisms of annular pressure on underground boreholes’ wellhead are similar to the high-pressure gas field, which could cause casing integrity failure [97]. Similar problems for the cases of horizontal wells are quite well known [98–100]; at the same time, the relationship of wells’ failure in connection with the pitch of the roof landing is covered rather modestly.

Clear parallels between the model results obtained from Figure 4 can be clearly seen with a sharp decline in the methane concentration in well #3 (see the Figure 17 study [84]) of Pingmei No. 8 Coal Mine. This pattern has been revealed due to the length of the channel, when changes in the stress–strain state of the massif do not affect the wellhead zones. Similar patterns are traced with the operation of well No. 3 (see Figure 4a) and panels E3 and E4 of Tabas Mine (Iran) [101], where the nonlinear character of methane emission curves is traced for both panels and with similar amplitude parameters. Also interesting are the changes in time of the S-shaped curves (Figure 3 of the study [102]) of methane concentration changes in the methane concentration during mining of Panel I-C (Staszic-Wujek Mine, Poland). Their generalized form when reflected in the true 3D form would be similar to the models obtained by us in the main part of the work.

Techniques for modeling multifactorial nonlinear dynamic processes are still imperfect. The application of stochastic algorithms, as well as those based on learning, does not always allow a sufficiently reliable confirmation of the quality consistency of the model with the experimental data, even with a preferential set of retrospective data. At the same time, deterministic methods make it possible, in some cases, to simplify multispectral or multistage processing of a discrete data set. Our three-dimensional models in the S-L statement (length from the beginning of the section distance to the face) [51] can extend the ideas about the stress–strain state of the roof in the mined-out area (models as Figure 6 from [103]), as well as the wave dynamics of pore pressure in gauges RP2 and RP3 above LW5121 (Anhui Province, China) [104]. A pronounced nonlinear character in combination with jumplike local bursts of methane emission dynamics is typical for both types of wells, indicating the discontinuity of deformation processes in the overlying rocks of the roof with the expansion of areas (shells) of zonal disintegration deep into the rock massif. Perhaps this can be explained by the presence of discontinuous deformation in the roof of a deep roadway, described in the work [83].

Moreover, one of the recent studies [105] convincingly proved the relationship between pressure release and the growth of methane concentration from 4 m after the longwall passage in the Tingnan Coal Mine (China). At the same time, the fact [106,107] that the dynamics of methane emission directly depends on changes in the concentration of gas in the extracted mixture indicates an obvious opportunity to use the latter as a “connecting link”. It can be effectively used for a qualitative assessment of the direct and inverse relationship between the stress–strain state of the geoenvironment and the distribution of gas flows in it.

The advantage of the author's approach is using the established patterns of the best natural stability of undermined wells to optimize the parameters of the spatial orientation of the existing drilling passport. Other methods of preliminary degassing (fishbone well or fracture, any preliminary action on the massif) (according to the general theory of degassing) are always more energy consuming than "advanced degassing" (when drilling of wells ends at 100–70 m immediately before the approach of the lava and their mouth is not yet deformed due to the effect of "zonal disintegration" of the massif in the area of influence of the drift) due to the fact that the natural unloading of the overlying rocks causes the transformation of the solid coal-gas solution with the intensification of the flow rate into zones of technogenic fracturing.

5. Conclusions

Increasing methane production from unconventional deposits to ensure decarbonization of coal mining is difficult to ensure without complicating approaches to modeling the distribution of gas flows in the goaf.

The scientific significance of the work lies in the ideas of development about the implementation mechanism and patterns of rock pressure nonlinear manifestations (the methane concentration dynamics in a mixture with a constant vacuum pressure is considered to be an indirect indicator of deformation process development), inducing the activation of methane release into underground wells, determining the parameters of drilling wells that provide greater natural stability and productivity of advanced drainage, but being more prone to failure during the primary roof breaks. As a result, the following main points were identified:

- It was found that a 50% increase in the inclination angle (from 40° to 60° with other drilling parameters being equal) leads to a uniform decrease in the productive work area distance (60%) from 13 to 5 m just before the roof landing, followed by a sharp increase in the area up to 35 m ahead of the face;
- If the inclination angle is 40°, the effect of advance degassing is characterized by significant irregularity, which is accompanied by nonlinear alternation of local maximums and minimums of methane emission, while the zone of productive work (ahead of the face) does not exceed 5 m before planting the roof, followed by a sharp but short-lived increase in distance to 40–42 m.

The practical significance of the results obtained lies in the use of established patterns to select the optimal parameters for drilling underground wells and ensure the safe development of coal and gas deposits. In these specific conditions, increasing the productivity of methane capturing from the technogenic disturbed coal-gas reservoir is more representative of the abandonment of all wells N° 3 and the transition to a more frequent grid of well clusters of wells N° 4. This, on the one hand, will increase the quality of "interception" of gas flow emission from the zone, anticipating fracturing by more remote wells; on the other hand, it will make the operation of the entire system more reliable. At the same time, it is necessary to develop a separate set of measures in the field of work at the mine in the conditions of shutdown of individual well clusters or emergency operation of the territory degassing network.

The universality of the obtained results consists in the possibility of expanding the use of the authors' approach to modeling nonlinear processes for a wider range of tasks, for example, to improve the methodology for presenting the results of "carbon polygons" [57,58] or assessing the impact of mining wastes on the environment [108–110].

The promising areas for further research are related to improving the methodology for obtaining qualitative 3D regression models (formulas) when processing "big smoothed data" based on teacher training (one of the standard machine learning methods) and comparing them with images of basic projections (Figure 4).

Author Contributions: Conceptualization, B.V.M. and V.I.G.; methodology, V.B.; software, V.V.K.; validation, Y.A.T. and A.A.B.; formal analysis, S.V.T.; investigation, V.B.; resources, V.V.K.; data

curation, Y.A.T.; writing—original draft preparation, V.B.; writing—review and editing, B.V.M. and V.I.G.; visualization, A.A.B.; supervision, B.V.M.; project administration, B.V.M. and V.I.G.; funding acquisition, Y.A.T. All authors have read and agreed to the published version of the manuscript.

Funding: The study was funded by the state assignment research of FRC SSC RAS FGRW-2021-0015, project N° 122032300363-3 (Brigida V., designing of the author’s approach to modeling nonlinear processes).

Data Availability Statement: The data presented in this study are available from the corresponding authors upon reasonable request.

Conflicts of Interest: The authors declare no conflict of interest.

References

- Singh, R.; Khan, S.; Dsilva, J. A framework for assessing critical factor for circular economy practice implementation. *J. Model. Manag.* **2022**, ahead of print. [CrossRef]
- Singh, R.; Khan, S.; Centobelli, P. Investigating the Interplay between Social Performance and Organizational Factors Supporting Circular Economy Practices. *Sustainability* **2022**, *14*, 16781. [CrossRef]
- Zhanbayev, R.A.; Yerkin, A.Y.; Shutaleva, A.V.; Irfan, M.; Gabelashvili, K.; Temirbaeva, G.R.; Chazova, I.Y.; Abdykadyrkyzy, R. State asset management paradigm in the quasi-public sector and environmental sustainability: Insights from the Republic of Kazakhstan. *Front. Environ. Sci.* **2023**, *10*, 1037023. [CrossRef]
- Martirosyan, A.V.; Ilyushin, Y.V. The Development of the Toxic and Flammable Gases Concentration Monitoring System for Coalmines. *Energies* **2022**, *15*, 8917. [CrossRef]
- Balovtsev, S.V. Higher rank aerological risks in coal mines. *Min. Sci. Technol.* **2022**, *7*, 310–319. [CrossRef]
- Dyachkova, M.A.; Novgorodtseva, A.N.; Tomyuk, O.N. Humanitarization of technical university education: Effective strategies and practices. *Perspekt. Nauki Obraz.* **2020**, *47*, 75–87. [CrossRef]
- Dvoynikov, M.V.; Leusheva, E.L. Modern trends in hydrocarbon resources development. *J. Min. Sci.* **2022**, *258*, 879–880. Available online: <https://pmi.spmi.ru/index.php/pmi/article/view/16101> (accessed on 26 April 2023).
- Ghorbani, Y.; Nwaila, G.T.; Zhang, S.E.; Bourdeau, J.E.; Cánovas, M.; Arzua, J.; Nikadat, N. Moving towards deep underground mineral resources: Drivers, challenges and potential solutions. *Resour. Policy* **2023**, *80*, 103222. [CrossRef]
- Huang, L.; Wang, S.; Cai, X.; Song, Z. Mathematical Problems in Rock Mechanics and Rock Engineering. *Mathematics* **2023**, *11*, 67. [CrossRef]
- Litvinenko, V. Advancement of geomechanics and geodynamics at the mineral ore mining and underground space development. In Proceedings of the Geomechanics and Geodynamics of Rock Masses At: International European Rock Mechanics Symposium (EUROCK), Saint Petersburg, Russia, 22–26 May 2018; pp. 3–18, WOSUID: WOS:000613258200001.
- Que, C.T.; Nevskaya, M.; Marinina, O. Coal Mines in Vietnam: Geological Conditions and Their Influence on Production Sustainability Indicators. *Sustainability* **2021**, *13*, 11800. [CrossRef]
- Zhong, S.; Lin, D. Evaluation of the Coordination Degree of Coal and Gas Co-Mining System Based on System Dynamics. *Sustainability* **2022**, *14*, 16434. [CrossRef]
- Borowski, M.; Zyczkowski, P.; Cheng, J.; Luczak, R.; Zwolinska, K. The Combustion of Methane from Hard Coal Seams in Gas Engines as a Technology Leading to Reducing Greenhouse Gas Emissions-Electricity Prediction Using ANN. *Energies* **2020**, *13*, 4429. [CrossRef]
- Tailakov, O.V.; Zastrellov, D.N.; Utkaev, E.A.; Smyslov, A.L.; Kormin, A.N. Experience for coal mine methane utilization to generate thermal and electric power. In Proceedings of the Taishan Academic Forum—Project on Mine Disaster Prevention and Control, Qingdao, China, 17–20 October 2014; pp. 450–453. [CrossRef]
- Smirnova, A.; Varnavskiy, K.; Nepsha, F.; Kostomarov, R.; Chen, S. The Development of Coal Mine Methane Utilization Infrastructure within the Framework of the Concept “Coal-Energy-Information”. *Energies* **2022**, *15*, 8948. [CrossRef]
- Li, Q.; Guo, J.; Zhang, C.; Yang, Y.; Ma, J.; Ren, Z. Research Findings on the Application of the Arch Structure Model in Coal Mining, a Review. *Sustainability* **2022**, *14*, 14714. [CrossRef]
- Khanal, M.; Adhikary, D.; Balusu, R.; Wilkins, A.; Belle, B. Mechanical study of shear failure of vertical goaf drainage hole. *Geotech. Geol. Eng.* **2022**, *40*, 1899–1920. [CrossRef]
- Rybak, J.; Khayrutdinov, M.M.; Kuziev, D.A.; Kongar-Syuryun, C.B.; Babyr, N.V. Prediction of the geomechanical state of the rock mass when mining salt deposits with stowing. *J. Min. Inst.* **2022**, *253*, 61–70. [CrossRef]
- Zhao, P.; Zhuo, R.; Li, S.; Shu, C.-M.; Jia, Y.; Lin, H.; Chang, Z.; Ho, C.-H.; Laiwang, B.; Xiao, P. Fractal characteristics of methane migration channels in inclined coal seams. *Energy* **2021**, *225*, 120127. [CrossRef]
- Karimpouli, S.; Tahmasebi, P.; Ramandi, H.L. A review of experimental and numerical modeling of digital coalbed methane: Imaging, segmentation, fractures modeling and permeability prediction. *Int. J. Coal Geol.* **2020**, *228*, 103552. [CrossRef]
- Ali, M.; Wang, E.; Li, Z.; Wang, X.; Khan, N.M.; Zang, Z.; Alarifi, S.S.; Fissaha, Y. Analytical Damage Model for Predicting Coal Failure Stresses by Utilizing Acoustic Emission. *Sustainability* **2023**, *15*, 1236. [CrossRef]

22. Liu, P.; Nie, B.; Zhao, Z.; Zhao, Y.; Li, Q. Characterization of ultrasonic induced damage on multi-scale pore/fracture in coal using gas sorption and μ -CT 3D reconstruction. *Fuel* **2023**, *332*, 126178. [[CrossRef](#)]
23. Guo, H.; Yuan, L.; Shen, B.; Qu, Q.; Xue, J. Mining-induced strata stress changes, fractures and gas flow dynamics in multi-seam longwall mining. *Int. J. Rock Mech. Min.* **2012**, *54*, 129–139. [[CrossRef](#)]
24. Zaalishvili, V.B.; Hasanov, A.B.; Abbasov, E.Y.; Mammadova, D.N. Detailing the Pore Structure of Productive Intervals of Oil Wells Using the Color 3D Imaging. *Energies* **2023**, *16*, 217. [[CrossRef](#)]
25. Zhang, Z.; Zhang, R.; Cao, Z.; Gao, M.; Zhang, Y.; Xie, J. Mechanical Behavior and Permeability Evolution of Coal under Different Mining Induced Stress Conditions and Gas Pressures. *Energies* **2020**, *13*, 2677. [[CrossRef](#)]
26. Brigida, V.S.; Zinchenko, N.N. Methane release in drainage holes ahead of coal face. *J. Min. Sci.* **2014**, *50*, 60–64. [[CrossRef](#)]
27. Wang, S.; Liu, K.; Wang, S.; Liang, Y.; Tian, F. Three-dimensional stochastic distribution characteristics of void fraction in longwall mining-disturbed overburden. *Bull. Eng. Geol. Environ.* **2022**, *81*, 414. [[CrossRef](#)]
28. Chen, S.G.; Guo, H. Numerical Simulation of Bed Separation Development and Grout Injection into Separations. *Geotech. Geol. Eng.* **2008**, *26*, 375–385. [[CrossRef](#)]
29. Qu, Q.; Guo, H.; Balusu, R. Methane emissions and dynamics from adjacent coal seams in a high permeability multi-seam mining environment. *Int. J. Coal Geol.* **2022**, *253*, 103969. [[CrossRef](#)]
30. Khanal, M.; Qu, Q.; Zhu, Y.; Xie, J.; Zhu, W.; Hou, T.; Song, S. Characterization of Overburden Deformation and Subsidence Behavior in a Kilometer Deep Longwall Mine. *Minerals* **2022**, *12*, 543. [[CrossRef](#)]
31. Wang, K.; Fu, Q.; Xu, C.; Zhao, C.; Zhao, W.; Yang, T. Influence of Coal Pillars on the Stress and Permeability of Mining-Disturbed Coal Seams for CBM Drainage. *Mining Metall. Explor.* **2022**, *39*, 2449–2459. [[CrossRef](#)]
32. Xu, C.; Wang, K.; Li, X.; Yuan, L.; Zhao, C.; Guo, H. Collaborative gas drainage technology of high and low level roadways in high-gassy coal seam mining. *Fuel* **2022**, *323*, 124325. [[CrossRef](#)]
33. Qin, Z.; Shen, H.; Yuan, Y.; Gong, Z.; Chen, Z.; Xia, Y. Determination of Gas Extraction Borehole Parameters in Fractured Zone on ‘Borehole in Place of Roadway’ Based on RSM-GRA-GA. *Processes* **2022**, *10*, 1421. [[CrossRef](#)]
34. Yang, Y.; Liu, S. Integrated modeling of multi-scale transport in coal and its application for coalbed methane recovery. *Fuel* **2021**, *300*, 120971. [[CrossRef](#)]
35. Wang, G.; Fan, C.; Xu, H.; Liu, X.; Wang, R. Determination of Long Horizontal Borehole Height in Roofs and Its Application to Gas Drainage. *Energies* **2018**, *11*, 2647. [[CrossRef](#)]
36. Damghani, M.; Rahmancejad, R.; Najafi, M. Evaluation of the Effect of Coal Seam Dip on Stress Distribution and Displacement around the Mechanized Longwall Panel. *J. Min. Sci.* **2019**, *55*, 733–742. [[CrossRef](#)]
37. Ma, H.; Yang, Y.; Chen, Z. Numerical simulation of bitumen recovery via supercritical water injection with in-situ upgrading. *Fuel* **2022**, *313*, 122708. [[CrossRef](#)]
38. Shang, Y.; Wu, G.; Liu, Q.; Kong, D.; Li, Q. The drainage horizon determination of high directional long borehole and gas control effect analysis. *Adv. Civ. Eng.* **2021**, *2021*, 3370170. [[CrossRef](#)]
39. Zhang, Q.; Wang, E.; Li, Z.; Wang, H.; Xue, Z. Control of directional long borehole on gas drainage and optimal design: Case study. *J. Nat. Gas Eng.* **2022**, *107*, 104766. [[CrossRef](#)]
40. Zuev, B.Y.; Zubov, V.P.; Fedorov, A.S. Application prospects for models of equivalent materials in studies of geotechnical processes in underground mining of solid minerals. *Eurasian Min.* **2019**, *1*, 8–12. [[CrossRef](#)]
41. Kachurin, N.M.; Stas, G.V.; Kachurin, A.N. Dynamics of gas emission from exposed surface of gas bearing coal seams having medium thickness. *Sustain. Dev. Mt. Territ.* **2021**, *3*, 441–448. (In Russian) [[CrossRef](#)]
42. Kazanin, O.I.; Sidorenko, A.A.; Sidorenko, S.A.; Ivanov, V.V.; Mischo, H. High productive longwall mining of multiple gassy seams: Best practices and recommendations. *Acta Montan. Slovaca* **2022**, *27*, 152–162. [[CrossRef](#)]
43. Liu, Y.K.; Shao, S.H.; Wang, X.X.; Chang, L.P.; Cui, G.L.; Zhou, F.B. Gas flow analysis for the impact of gob gas ventholes on coalbed methane drainage from a longwall gob. *J. Nat. Gas Sci. Eng.* **2016**, *36*, 1312–1315. [[CrossRef](#)]
44. Xiao, P.; Liu, X.; Zhao, B. Experimental study on gas adsorption characteristics of coals under different Protodyakonov’s coefficient. *Energy Rep.* **2022**, *8*, 10614–10623. [[CrossRef](#)]
45. Szlazak, N.; Obracaj, D.; Korzec, M. Estimation of Gas Loss in Methodology for Determining Methane Content of Coal Seams. *Energies* **2021**, *14*, 982. [[CrossRef](#)]
46. Li, Q.; Xu, J.; Yan, F.; Peng, S.; Zhang, C.; Zhang, X. Evolution characteristics of reservoir parameters during coalbed methane drainage via in-seam horizontal boreholes. *Powder Technol.* **2020**, *362*, 591–603. [[CrossRef](#)]
47. Peng, S.; Jia, L.; Xu, J.; Zhang, C.; Li, Q.; Han, E. The production schedule optimization of a multilayer superposed CBM system: An experimental study. *Powder Technol.* **2020**, *373*, 99–108. [[CrossRef](#)]
48. Zhang, C.; Xu, J.; Wang, E.; Peng, S. Experimental Study on the Gas Flow Characteristics and Pressure Relief Gas Drainage Effect under Different Unloading Stress Paths. *Geofluids* **2020**, *8*, 8837962. [[CrossRef](#)]
49. Zhao, W.; Wang, K.; Zhang, R.; Dong, H.; Lou, Z.; An, F. Influence of combination forms of intact sub-layer and tectonically deformed sub-layer of coal on the gas drainage performance of boreholes: A numerical study. *Int. J. Coal Sci. Technol.* **2020**, *7*, 571–580. [[CrossRef](#)]
50. Kubrin, S.S.; Tailakov, O.V.; Sobolev, V.V.; Zakharov, V.N. The use of the Allan variation in the processing of the measured parameters of the methane-air mixture during the degassing of excavation sites. *Ugol* **2022**, *12*, 60–66. (In Russian) [[CrossRef](#)]

51. Brigida, V.S.; Golik, V.I.; Dzeranov, B.V. Modeling of Coalmine Methane Flows to Estimate the Spacing of Primary Roof Breaks. *Mining* **2022**, *2*, 809–821. [[CrossRef](#)]
52. Klyuev, R.V.; Morgoev, I.D.; Morgoeva, A.D.; Gavrina, O.A.; Martyushev, N.V.; Efremkov, E.A.; Mengxu, Q. Methods of Forecasting Electric Energy Consumption: A Literature Review. *Energies* **2022**, *15*, 8919. [[CrossRef](#)]
53. Kabanov, E.I.; Korshunov, G.I.; Gridina, E.B. Algorithmic provisions for data processing under spatial analysis of risk of accidents at hazardous production facilities. *Nauk. Visnyk Natsionalnoho Hirnychoho Universytetu* **2019**, *6*, 117–121. [[CrossRef](#)]
54. Iakovleva, E.; Belova, M.; Soares, A.; Rassölkina, A. On the Issues of Spatial Modeling of Non-Standard Profiles by the Example of Electromagnetic Emission Measurement Data. *Sustainability* **2022**, *14*, 574. [[CrossRef](#)]
55. Isametova, M.E.; Nussipali, R.; Martyushev, N.V.; Malozyomov, B.V.; Efremkov, E.A.; Isametov, A. Mathematical Modeling of the Reliability of Polymer Composite Materials. *Mathematics* **2022**, *10*, 3978. [[CrossRef](#)]
56. Bosikov, I.I.; Klyuev, R.V.; Azhmukhamedov, I.M.; Revazov, V.C. Statistical dynamics-based estimation of ventilation control in coal mines. *Min. Inf. Anal. Bull.* **2021**, *11*, 123–135. (In Russian) [[CrossRef](#)]
57. Guo, Q.; Peng, H.; Hong, B.; Yao, H.; Zhu, Y.; Ding, H.; An, N.; Hong, Y. Variations of methane stable isotopic values from an Alpine peatland on the eastern Qinghai-Tibetan Plateau. *Acta Geochim.* **2021**, *40*, 473–483. [[CrossRef](#)]
58. Yao, H.; Peng, H.; Hong, B.; Guo, Q.; Ding, H.; Hong, Y.; Zhu, Y.; Cai, C.; Chi, J. Environmental Controls on Multi-Scale Dynamics of Net Carbon Dioxide Exchange From an Alpine Peatland on the Eastern Qinghai-Tibet Plateau. *Front. Plant Sci.* **2022**, *12*, 791343. [[CrossRef](#)]
59. Khan, S.A. Trigonometric ratios using algebraic methods. *Math. Stat.* **2021**, *9*, 899–907. [[CrossRef](#)]
60. Vorobieva, I.A.; Gvishiani, A.D.; Dzeboev, B.A.; Dzeranov, B.V.; Barykina, Y.V.; Antipova, A.O. Nearest Neighbor Method for Discriminating Aftershocks and Duplicates When Merging Earthquake Catalogues. *Front. Earth Sci.* **2022**, *10*, 820277. [[CrossRef](#)]
61. Zaalishvili, V.; Burdzieva, O.; Kanukov, A.; Zaks, T. Eco-Geophysical and Geocological Factors in Assessing the State of the Geological Environment Based on the Analysis of Spatial Databases of the Territory of the Republic of North Ossetia-Alania. *Appl. Sci.* **2022**, *12*, 2644. [[CrossRef](#)]
62. Dai, L.; Lei, H.; Cheng, X.; Li, R. Prediction of coal seam gas content based on the correlation between gas basic parameters and coal quality indexes. *Front. Energy Res.* **2023**, *10*, 1096539. [[CrossRef](#)]
63. Zaki, M.M.; Chen, S.; Zhang, J.; Feng, F.; Khoreshok, A.A.; Mahdy, M.A.; Salim, K.M. A Novel Approach for Resource Estimation of Highly Skewed Gold Using Machine Learning Algorithms. *Minerals* **2022**, *12*, 900. [[CrossRef](#)]
64. Jafarpour, A.; Najafi, M. Selection of Compatible Coal Seam for Methane Drainage Operation Based on Uncertain Geological Conditions: A Hybrid Fuzzy Approach. *Math. Probl. Eng.* **2022**, *2022*, 4586979. [[CrossRef](#)]
65. Naveen, N.S.; Kishore, P.S.; Pujari, S.; Silas Kumar, M.D.; Jogi, K. Optimization through Taguchi and artificial neural networks on thermal performance of a radiator using graphene-based coolant. *Proc. Inst. Mech. Eng. A J. Power Energy* **2022**, *236*, 1680–1693. [[CrossRef](#)]
66. Adero, N.J.; Drebenstedt, C.; Prokofeva, E.N.; Vostrikov, A.V. Spatial data and technologies for geomonitoring of land use under aspect of mineral resource sector development. *Eurasian Min.* **2020**, *1*, 69–74. [[CrossRef](#)]
67. Lipilin, D.A.; Evtushenko, D.D. Assessment of the urban environment quality using geoinformation systems by the example of microdistricts of the city of Krasnodar. *Russ. Geol. Geophys.* **2022**, *12*, 195–210. (In Russian) [[CrossRef](#)]
68. Skripchinsky, A.V.; Badov, A.D.; Badov, O.A.; Borisov, D.D. Water protection zone state analysis of the Derbent city district on the basis of GIS technologies. *Russ. Geol. Geophys.* **2022**, *12*, 180–192. (In Russian) [[CrossRef](#)]
69. Golik, V.I.; Dmitrak, Y.V.; Brigida, V.S. Impact of duration of mechanochemical activation on enhancement of zinc leaching from polymetallic ore tailings. *Nauk. Visnyk Natsionalnoho Hirnychoho Universytetu* **2020**, *1*, 47–54. [[CrossRef](#)]
70. Qin, B.; Shi, Z.S.; Hao, J.F.; Ye, D.L.; Liang, B.; Sun, W.J. Analysis of the Space–Time Synergy of Coal and Gas Co-mining. *ACS Omega* **2022**, *7*, 13737–13749. [[CrossRef](#)]
71. Gutarevich, V.O.; Martyushev, N.V.; Klyuev, R.V.; Kukartsev, V.A.; Kukartsev, V.V.; Iushkova, L.V.; Korpacheva, L.N. Reducing Oscillations in Suspension of Mine Monorail Track. *Appl. Sci.* **2023**, *13*, 4671. [[CrossRef](#)]
72. Efremkov, E.A.; Martyushev, N.V.; Skeebea, V.Y.; Grechneva, M.V.; Olisov, A.V.; Ens, A.D. Research on the Possibility of Lowering the Manufacturing Accuracy of Cycloid Transmission Wheels with Intermediate Rolling Elements and a Free Cage. *Appl. Sci.* **2022**, *12*, 5. [[CrossRef](#)]
73. Li, J.; Xuan, D.; Xu, J.; Dong, Z.; Wang, C. Compaction Response of Mining-Induced Rock Masses to Longwall Overburden Isolated Grouting. *Minerals* **2023**, *13*, 633. [[CrossRef](#)]
74. Dzhioeva, A.K.; Brigida, V.S. Spatial non-linearity of methane release dynamics in underground boreholes for sustainable mining. *J. Min. Inst.* **2020**, *245*, 522–530. [[CrossRef](#)]
75. Zhao, P.; An, X.; Li, S.; Kang, X.; Huang, Y.; Yang, J.; Jin, S. Study on the Pseudo-Slope Length Effect of Buried Pipe Extraction in Fully Mechanized Caving Area on Gas Migration Law in Goaf. *Sustainability* **2023**, *15*, 6628. [[CrossRef](#)]
76. Nepsha, F.S.; Voronin, V.A.; Liven, A.S.; Korneev, A.S. Feasibility study of using cogeneration plants at Kuzbass coal mines. *J. Min. Inst.* **2023**, *259*, 141–150. [[CrossRef](#)]
77. Li, J.; Liu, S.; Ren, W.; Liu, H.; Li, S.; Yan, K. Research on Engineering Practice and Effect Evaluation Method of Pressure Relief in Deep Rock Burst Danger Area of Coal Mine. *Minerals* **2023**, *13*, 570. [[CrossRef](#)]
78. Montano, J.; Coco, G.; Antolinez, J.A.A.; Beuzen, T.; Bryan, K.R.; Cagigal, L.; Castelle, B.; Davidson, M.A.; Goldstein, E.B.; Ibaceta, R.; et al. Blind testing of shoreline evolution models. *Sci. Rep.* **2020**, *10*, 2137. [[CrossRef](#)]

79. Ali, G.; Sajjad, M.; Kanwal, S.; Xiao, T.; Khalib, S.; Shoaib, F.; Gul, H.N. Spatial–temporal characterization of rainfall in Pakistan during the past half-century (1961–2020). *Sci. Rep.* **2021**, *11*, 6935. [[CrossRef](#)]
80. Chicco, D.; Warrens, M.J.; Jurman, G. The coefficient of determination R-squared is more informative than SMAPE, MAE, MAPE, MSE and RMSE in regression analysis evaluation. *PeerJ Comput. Sci.* **2021**, *7*, e623. [[CrossRef](#)]
81. Golik, V.I.; Klyuev, R.V.; Martyushev, N.V.; Brigida, V.; Efremkov, E.A.; Sorokova, S.N.; Mengxu, Q. Tailings Utilization and Zinc Extraction Based on Mechanochemical Activation. *Materials* **2023**, *16*, 726. [[CrossRef](#)]
82. Massaoudi, M.S.; Refaat, S.; Abu-Rub, H.; Chihi, I.; Oueslati, F.S. PLS-CNN-BiLSTM: An End-to-End Algorithm-Based Savitzky-Golay Smoothing and Evolution Strategy for Load Forecasting. *Energies* **2020**, *13*, 5464. [[CrossRef](#)]
83. Han, C.; Zhang, N.; Yang, H.; Liu, J.; Zhao, Q.; Huo, Y.; Song, K. Discontinuous deformation characteristics of deep buried roadway roof and linkage control of thick layer cross-boundary anchorage: A Case Study. *Energies* **2023**, *15*, 2806. [[CrossRef](#)]
84. Zhang, F.; Wang, G.; Wang, B. Study and Application of High-Level Directional Extraction Borehole Based on Mining Fracture Evolution Law of Overburden Strata. *Sustainability* **2023**, *15*, 2806. [[CrossRef](#)]
85. Cao, L.; Sun, J.; Zhang, B.; Lu, N.; Xu, Y. Sensitivity analysis of the temperature profile changing law in the production string of a high-pressure high-temperature gas well considering the coupling relation among the gas flow friction, gas properties, temperature, and pressure. *Front. Phys.* **2022**, *10*, 1050229. [[CrossRef](#)]
86. Zhang, H.; Cheng, Y.; Yuan, L.; Wang, L.; Jiang, J.; Li, G. Gas extraction challenge and the application of hydraulic cavity technology in the Shijiazhuang coalmine, Qinshui basin. *Energy Sources A Recovery Util. Environ. Eff.* **2019**, *43*, 1–23. [[CrossRef](#)]
87. Niu, Y.; Zhang, X.; Wang, E.; Li, Z.; Cheng, Z.; Duan, X.; Li, H.; Wei, Y.; Qian, J.; Cai, G.; et al. A new method of monitoring the stability of boreholes for methane drainage from coal seams. *Meas. J. Int. Meas. Confed.* **2020**, *154*, 107521. [[CrossRef](#)]
88. Qu, Q.; Guo, H.; Khanal, M. Monitoring and analysis of ground movement from multi-seam mining. *Int. J. Rock Mech. Min.* **2021**, *148*, 104949. [[CrossRef](#)]
89. Brigida, V.S.; Dmitrak, Y.V.; Gabaraev, O.Z.; Golik, V.I. Use of destressing drilling to ensure safety of Donbass gas-bearing coal seams extraction. *Occup. Saf. industry.* **2019**, *3*, 7–11. (In Russian) [[CrossRef](#)]
90. Liu, Y.; Chang, L.; Zhou, F.; Tan, D.; Liu, L.; Kang, J.; Tian, H. Numerical modeling of gas flow in deformed well casing for the prediction of local resistance coefficients pertinent to longwall mining and its engineering evaluation. *Environ. Earth. Sci.* **2017**, *76*, 686. [[CrossRef](#)]
91. Kunshin, A.; Dvoynikov, M.; Timashev, E.; Starikov, V. Development of Monitoring and Forecasting Technology Energy Efficiency of Well Drilling Using Mechanical Specific Energy. *Energies* **2022**, *15*, 7408. [[CrossRef](#)]
92. Dzhioeva, A.K. Improvement of Underground Leaching Technology while Ensuring Environmentally Safe Development of Ore Deposits. *Occup. Saf. industry.* **2022**, *9*, 62–68. (In Russian) [[CrossRef](#)]
93. Rakishev, B.; Kenzhetaev, Z.; Mataev, M.; Togizov, K. Improving the Efficiency of Downhole Uranium Production Using Oxygen as an Oxidizer. *Minerals* **2022**, *12*, 1005. [[CrossRef](#)]
94. Bosikov, I.I.; Klyuev, R.V.; Mayer, A.V. Comprehensive assessment of hydraulic fracturing technology efficiency for well construction during hydrocarbon production. *J. Min. Inst.* **2022**, *258*, 1018–1025. [[CrossRef](#)]
95. Čečko, J.; Urych, T.; Magdziarczyk, M.; Smolinski, A. Research on the Processes of Injecting CO₂ into Coal Seams with CH₄ Recovery Using Horizontal Wells. *Energies* **2020**, *13*, 416. [[CrossRef](#)]
96. Brigida, V.S.; Golik, V.I.; Dmitrak, Y.V.; Gabaraev, O.Z. Ensuring Stability of Undermining Inclined Drainage Holes During Intensive Development of Multiple Gas-Bearing Coal Layers. *J. Min. Inst.* **2019**, *239*, 497–501. [[CrossRef](#)]
97. Cao, L.; Sun, J.; Zhang, B.; Lu, N.; Xu, Y. Analysis of Multiple Annular Pressure in Gas Storage Well and High-Pressure Gas Well. *Energy Eng.* **2023**, *120*, 35–48. [[CrossRef](#)]
98. Bosikov, I.I.; Egorova, E.V.; Karpikov, A.V. Estimation of the optimal direction of the horizontal borehole relative to the minimum and maximum formation stress. *IOP Conf. Ser. Earth Environ. Sci.* **2022**, *1021*, 012066. [[CrossRef](#)]
99. Slastunov, S.; Kolikov, K.; Batugin, A.; Sadov, A.; Khautiev, A. Improvement of Intensive In-Seam Gas Drainage Technology at Kirova Mine in Kuznetsk Coal Basin. *Energies* **2022**, *15*, 1047. [[CrossRef](#)]
100. Hosseini, A.; Najafi, M. Determination of methane desorption zone for the design of a drainage borehole pattern (case study: E4 panel of the tabas mechanized coal mine, Iran). *Rud. Geol. Naft. Zb.* **2021**, *36*, 61–75. [[CrossRef](#)]
101. Hosseini, A.; Najafi, M.; Hossein Morshedy, A. Determination of suitable distance between methane drainage stations in Tabas mechanized coal mine (Iran) based on theoretical calculations and field investigation. *J. Min. Inst.* **2022**, *258*, 1050–1060. [[CrossRef](#)]
102. Leśniak, G.; Brunner, D.J.; Topór, T.; Słota-Valim, M.; Cicha-Szot, R.; Jura, B.; Skiba, J.; Przystolik, A.; Lyddall, B.; Plonka, G. Application of long-reach directional drilling boreholes for gas drainage of adjacent seams in coal mines with severe geological conditions. *Int. J. Coal Sci. Technol.* **2022**, *9*, 88. [[CrossRef](#)]
103. Li, H.; Liu, Y.; Wang, W.; Liu, M.; Ma, J.; Guo, X.; Guo, H. The integrated drainage technique of directional high-vel borehole of super large diameter on roof replacing roof extraction roadway: A case study of the underground Zhaozhuang Coal Mine. *Energy Rep.* **2020**, *6*, 2651–2666. [[CrossRef](#)]
104. Qu, Q.; Guo, H.; Yuan, L.; Shen, B.; Yu, G.; Qin, J. Rock Mass and Pore Fluid Response in Deep Mining: A Field Monitoring Study at Inclined Longwalls. *Minerals* **2022**, *12*, 463. [[CrossRef](#)]
105. Shi, Z.; Ye, D.; Hao, J.; Qin, B.; Li, G. Research on Gas Extraction and Cut Flow Technology for Lower Slice Pressure Relief Gas under Slice Mining of Extra-Thick Coal Seam. *ACS Omega* **2022**, *7*, 24531–24550. [[CrossRef](#)] [[PubMed](#)]

106. Zhang, C.; Song, Z.; Bai, Q.; Zhang, L.; Chen, J. Intensive field measurements for characterizing the permeability and methane release with the treatment process of pressure-relief mining. *Sci. Rep.* **2022**, *12*, 14847. [[CrossRef](#)] [[PubMed](#)]
107. Bosikov, I.I.; Martyushev, N.V.; Klyuev, R.V.; Savchenko, I.A.; Kukartsev, V.V.; Kukartsev, V.A.; Tynchenko, Y.A. Modeling and Complex Analysis of the Topology Parameters of Ventilation Networks When Ensuring Fire Safety While Developing Coal and Gas Deposits. *Fire* **2023**, *6*, 95. [[CrossRef](#)]
108. Kou, X.; Han, D.; Cao, Y.; Shang, H.; Li, H.; Zhang, X.; Yang, M. Acid Mine Drainage Discrimination Using Very High Resolution Imagery Obtained by Unmanned Aerial Vehicle in a Stone Coal Mining Area. *Water* **2023**, *15*, 1613. [[CrossRef](#)]
109. Plotnikova, N.V.; Skeebe, V.Y.; Martyushev, N.V.; Miller, R.A.; Rubtsova, N.S. Formation of high-carbon abrasion-resistant surface layers when high-energy heating by high-frequency currents. *IOP Conf. Ser. Mater. Sci. Eng.* **2016**, *156*, 012022. [[CrossRef](#)]
110. Kříbek, B.; Nyambe, I.; Sracek, O.; Mihaljevič, M.; Knésl, I. Impact of Mining and Ore Processing on Soil, Drainage and Vegetation in the Zambian Copperbelt Mining Districts: A Review. *Minerals* **2023**, *13*, 384. [[CrossRef](#)]

Disclaimer/Publisher's Note: The statements, opinions and data contained in all publications are solely those of the individual author(s) and contributor(s) and not of MDPI and/or the editor(s). MDPI and/or the editor(s) disclaim responsibility for any injury to people or property resulting from any ideas, methods, instructions or products referred to in the content.